

## UV–Vis Spectroscopic Trends of Liquid-exfoliated Graphite/ Graphene Nanoplatelets/Bioactive Glass Mixtures

Mohd Aiman Hakimi Abdul Rahim,<sup>1</sup> Siti Fatimah Samsurrijal,<sup>2</sup> Amirul Al-Ashraf  
Abdullah<sup>1</sup> and Siti Noor Fazliah Mohd Noor<sup>2\*</sup>

<sup>1</sup>School of Biological Sciences, Universiti Sains Malaysia, 11800 USM,  
Pulau Pinang, Malaysia

<sup>2</sup>Advanced Medical and Dental Institute, Universiti Sains Malaysia, 13200 Kepala Batas,  
Pulau Pinang, Malaysia

\*Corresponding author: fazliah@usm.my

Published online: 25 August 2023

To cite this article: Abdul Rahim, M. A. H. et al. (2023). UV–Vis spectroscopic trends of liquid-exfoliated graphite/graphene nanoplatelets/bioactive glass mixtures. *J. Phys. Sci.*, 34(2), 1–12. <https://doi.org/10.21315/jps2023.34.2.1>

To link to this article: <https://doi.org/10.21315/jps2023.34.2.1>

**ABSTRACT:** *Liquid-phase exfoliation of graphene using a suitable solvent is safe, although the sonication period needs further exploration, which may affect the exfoliation process. This study investigated graphene exfoliation in chloroform through UV–Vis spectroscopy. Graphite powder at different ratios was soaked in chloroform and sonicated at different sonication times from 30 min to 180 min and then subjected to centrifugation at 4,000 rpm for 30 min. The supernatant was collected and analysed using UV–Vis spectroscopy at wavelengths between 220 nm and 800 nm. The UV absorbance intensity showed that the presence of exfoliated graphene peaks is free of interference at 120 min. A comparative study was conducted by using graphene in chloroform as controls and adding bioactive glass (BG) within graphite powder-chloroform emulsions in different concentrations at 120 min. Graphene appearance at the anticipated absorption peak at ~270 nm was observed, and BG addition led to agglomeration, which could provide an idea for a better material formulation strategy in developing films that combined graphene/BG because of their exceptional properties suitable for diverse potential biomedical application.*

**Keywords:** graphite, graphene, bioactive glass, liquid-phase exfoliation, UV–Vis

## 1. INTRODUCTION

Graphene is a new topic in carbon nanoscience field. Novoselov and colleagues were amongst the pioneers to efficiently recover a single graphene sheet.<sup>1</sup> Naturally, graphene consists of a single thick planar two-dimensional layer that shows a honeycomb or hexagonal lattice structure comprising  $sp^2$ -hybridised carbon atoms. Individual graphene demonstrates unique properties by having excellent electron mobility of  $\sim 2.5 \times 10^5 \text{ cm}^2/\text{volt}\cdot\text{second}$  (V.s), high specific surface area of  $\sim 2,630 \text{ m}^2\text{g}^{-1}$ , Young modulus of  $\sim 1,000 \text{ GPa}$ , thermal conductivity of  $\sim 5,000 \text{ Wm}^{-1}\text{K}^{-1}$  and fascinating optical properties.<sup>2,3</sup> Graphene shows a great application potential as a next-generation biomaterial in numerous high-value applications including supercapacitors, energy storage, sensors, nanocomposites and coatings.<sup>3-7</sup> Graphene-based products in the biomedical field exist from drug delivery and biosensors to biomedical devices for medical and bioengineering applications.<sup>8</sup> Research on graphene as well as effort by various global institutions, where the National Graphene Association (USA) and the National Graphene Institute (UK) were established to promote graphene commercialisation, are persistently growing.<sup>9</sup> Malaysia also set up the National Graphene Action Plan 2020. However, the synthesis and production of graphene at a large scale remain a challenging task for researchers and manufacturers. The production of graphene can be divided into two types, which are bottom-up or top-down. In bottom-up operation, graphene is synthesised by the conversion of carbon precursors, including aromatic hydrocarbons, carbon-bearing gases and polymers, using a scalable method such as chemical vapour deposition, epitaxial growth, laser and thermal pyrolysis. These approaches are complexed because of the involvement of sophisticated infrastructure and high working temperatures, thereby limiting their applicability.<sup>10</sup> The top-down production has lower costs by transposing graphite to graphene via chemical oxidation–reduction, solid-phase exfoliation, liquid-phase exfoliation (LPE), electrochemical exfoliation and arc-discharge methods. However, these methods produce graphene with structural defects and low percentage of recovery.<sup>11</sup> The top-down method through LPE is a straightforward approach to disperse mono-layer or multi-layer defect-free and impurity-free graphene from graphite in a suitable solvent solution by sonicating graphitic materials at a relatively high concentration.<sup>12</sup> Sonication transmits ultrasonic waves, which produce cavitation bubbles that lessen the Van der Waals forces, thereby creating extensive interlayer spaces within the layers of the non-exfoliated graphite.<sup>10,12</sup> Various organic solvents are studied for LPE, such as N-Methyl-2-Pyrrolidone, N,N-Dimethylformamide and chloroform; chloroform is an excellent solvent candidate for graphene exfoliation because of its suitable surface energy, which is close to  $30 \text{ mJ/m}^2$ – $50 \text{ mJ/m}^2$ .<sup>13,14</sup> Excellent solvents are used to dissipate graphene, minimising the interfacial tension between the solvent

and graphene particles; thus, exfoliated graphene isolated in the solvent remains stable. The efficiency of graphene exfoliation depends on the used solvent, where each solvent necessitates a particular timing for sonication, thereby producing graphene at several concentrations.<sup>15</sup>

Bioactive glass (BG) has biodegradability, biocompatibility, bioactivity, antibacterial and anti-inflammatory properties.<sup>16</sup> BG dissolves and releases calcium and phosphorus ions under physiological conditions, and then such ions precipitate to develop a layer of hydroxyl carbonate apatite on its surface. Given the complexity and nano-scale of this layer, it can support the adsorption of adhesive proteins to induce angiogenesis.<sup>17,18</sup> At present, the use and modification of BG have been the highlight as BG possesses a natural brittle structure, which provides a great application potential to many sectors. The distinct characteristics of BG could assist and enhance cell attachment independently, and it can be functionalised into other biomaterials. Hence, the current project describes graphene exfoliation from graphite powder in chloroform at different weight percentages (wt%) by using the LPE method alongside a supplementary report on the sonication period. This project will provide a relative insight into the absorbance peak via UV–Vis analyses between exfoliated and pure graphene. Furthermore, BG is combined with graphite powder in a chloroform suspension and evaluated to recognise its application in materials science and biomedical field.

## **2. EXPERIMENTAL**

### **2.1 Liquid-Phase Exfoliation of Graphene**

Graphite powders (Supelco, Darmstadt, Germany) at different weight percentages (1.0 wt%, 3.0 wt% and 6.0 wt%) in chloroform (Sigma Aldrich, UK) were sonicated at different sonication times (30 min, 60 min, 120 min and 180 min) by using a tabletop bath sonicator at room temperature (Bandelin, Sonorex). The solvent volume was kept constant (10 mL) for all experiments. After sonication, the resultant suspension was further centrifuged at 4,000 rpm for 30 min (Eppendorf 5810R, Germany) to produce homogenous graphene sheet suspension in the chloroform. Pure graphene (Acros Organics, Geel, Belgium) was prepared as a comparative control. The supernatant was collected for all mixtures, and the absorbance intensity of exfoliated graphene suspensions was analysed using a UV–Vis spectrometer (FluoSTAR Omega, BMG Labtech, Germany). The presence of peaks in the suspension was determined at a wavelength between 220 nm and 800 nm, with chloroform as the background inside a 96-well plate with quadruplicates for each sample.

## 2.2 Preparation of BG Suspension

Sol-gel derived BG powder with a particle size less than 50  $\mu\text{m}$  was dissolved in chloroform at various concentrations of 1.0 wt%, 2.5 wt%, 5.0 wt%, 7.5 wt% and 10.0 wt%.<sup>18</sup> BG suspension was obtained by dispersing the mixtures via bath sonication for 120 min before centrifugation at 4,000 rpm for 30 min.

## 2.3 Preparation of Graphene and BG Suspension

Graphite powder (1.0 wt%, 3.0 wt% and 6.0 wt%) was mixed with BG powder (1.0 wt%, 2.5 wt% and 5.0 wt%) in the chloroform, and these suspensions were subjected to liquid exfoliation inside a bath sonicator for 120 min and subsequently centrifuged at 4,000 rpm for 30 min.

# 3. RESULTS AND DISCUSSION

## 3.1 Optimisation of Sonication Time

The optimisation of a technical parameter, which is the sonication time, was studied to determine the efficient sonication time whereby the mixture of graphite-solvent concentration, centrifugation period and centrifugation speed were fixed to detect the presence of graphene in the emulsion and to compare the absorbance intensity amongst various sonication time (30 min, 60 min, 120 min and 180 min). The peaks of graphene intensity exfoliated in chloroform for different sonication time using various concentrations of graphite powder (1.0 wt%, 3.0 wt% and 6.0 wt%; Figure 1) where the results show a prominent and narrow peak between 277 nm and 280 nm, which corresponded to a graphene peak.<sup>10</sup> With regard to the peak intensity, each of the graphite concentration showed an increasing trend as the sonication time increases from 30 min to 180 min. Nevertheless, the graphite powder at 6.0 wt% showed almost similar intensity when sonicated from 30 min to 180 min. The sonication time for a large amount of graphite demands a longer period (>180 min) or increases the energy of sonication; thus, the conversion of graphite to graphene can be improved. In addition, the presence of an absorption peak at  $\sim 279$  nm wavelength with the highest intensity at 120 min and 180 min for every concentration of graphite indicated successful graphene exfoliation. Meanwhile, 30 min of sonication is not efficient enough to exfoliate graphene from graphite because less energy had been provided. Thus, the sonication time for liquid exfoliation of graphene was set to 120 min as an optimum period to acquire our target material.

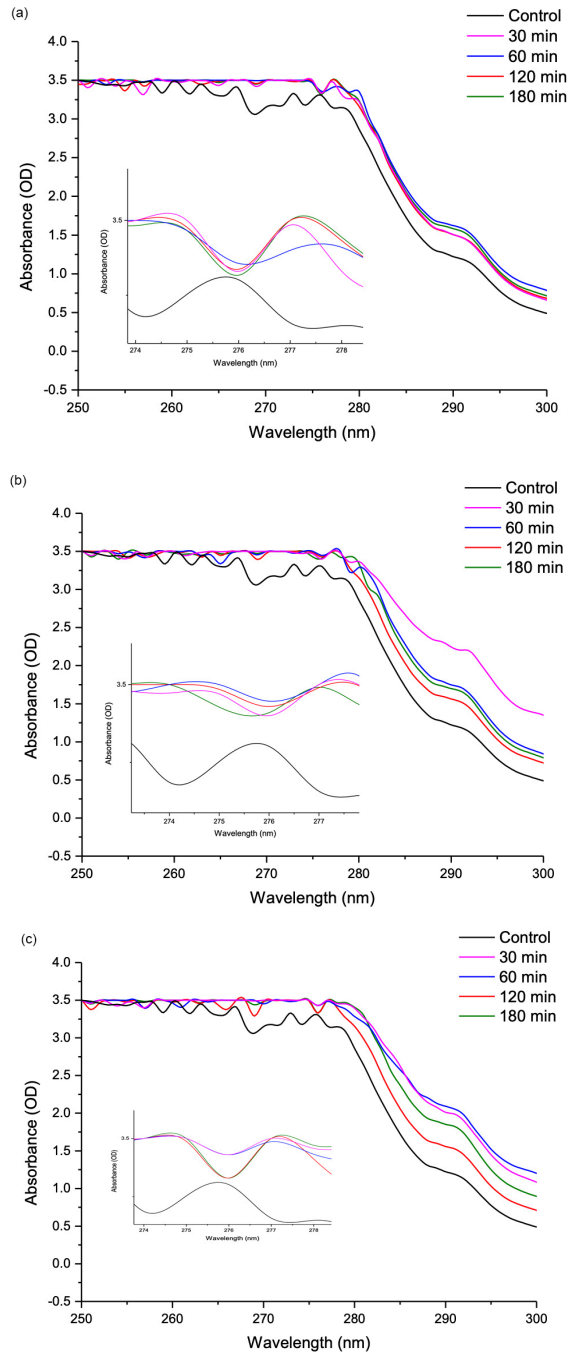


Figure 1: UV absorbance intensity of different weight percentages of liquid-exfoliated graphene in chloroform at different sonication time from 30 min to 180 min. (a) 1.0 wt%, (b) 3.0 wt% and (c) 6.0 wt%.

This study also compared the observed peaks with pure graphene to confirm the presence of a graphene sheet in the solvent suspension. Pure graphene flakes were sonicated for 120 min, and the UV-Vis trend of pure graphene shown in Figure 2 shows the presence of a peak at  $\sim 278$  nm, indicating the successful exfoliation of graphene. Based on a previous study, increasing the bath sonication time increases the absorption intensity, which indicates a high graphene concentration in the mixtures whereby the colour of the suspension mixture darkens after 120 min of sonication, thereby highlighting a greater extent of graphene exfoliation.<sup>19</sup> Our results demonstrated that the production of graphene at lower sonication time (120 min), resolving between quantity and cost, is achievable in chloroform because the properties of solvent are crucial for graphene exfoliation. The key for good solvent is characterised by its surface energy. In this case, the surface energy of chloroform is close to the literature values of the nanotube/graphite surface energy (i.e.,  $30 \text{ mJ/m}^2$ – $50 \text{ mJ/m}^2$ ). Chloroform assists and dissipates graphene to minimise the interfacial tension between the solvent and graphene particles; thus, exfoliated graphene isolated in the solvent remains stable.<sup>14,15</sup>

The exfoliation of graphene in the solvent occurs because of the vigorous interaction between the solvent molecules and graphite basal planes caused by external driving forces from sonication, thereby overcoming the energetic penalty and Van der Waals attractions amongst adjacent layers of graphite.<sup>20,21</sup>

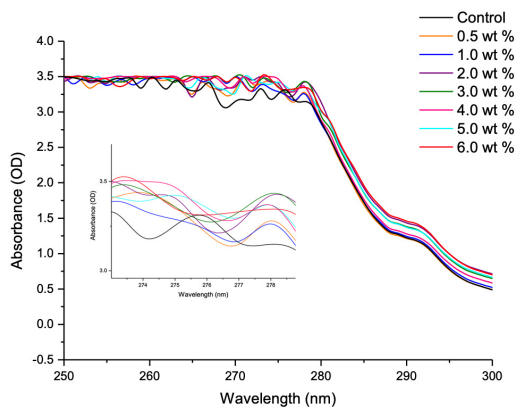


Figure 2: UV absorbance intensity of different weight percentages of pure graphene in chloroform following sonication at 120 min.

### 3.2 Determination of Graphene Concentration in Liquid Suspension

In this section, the concentration of exfoliated graphene from graphite powder was optimised after sonication for 120 min. Furthermore, the concentration of BG powder in chloroform sonicated for 120 min was carried out to combine

exfoliated graphene and BG as the next step in the process. Figure 3 shows absorbance intensity peaks of various concentrations of liquid-exfoliated graphene in chloroform. The absorbance peaks can be observed at  $\sim 279$  nm, which is almost similar to pure graphene (Figure 2). The presence of the peak indicates graphene dispersion for all concentrations of graphite powder that is related to the characteristic  $\pi-\pi^*$  transition of graphene/graphite and conjugation network of C-O bonds of graphene.<sup>22–24</sup> Moreover, the absorption spectrum between 300 nm and 800 nm is flat and featureless, which suggests an impurity-free material. The UV trend tends to increase as the weight percentage of the graphite powder increases from 1.0 wt% to 6.0 wt% in which the 1.0 wt% concentration has a less number of graphite particles absorbing the energy; thus, less efficient exfoliation of graphene was observed. Meanwhile, graphite at 3.0 wt% and 6.0 wt% has the optimum concentration as more energy can be adsorbed, and each graphite particle receives sufficient energy with slight agglomeration. The Van der Waals forces created between the solvent and particle are important to the entanglement process in which low force tends to halt dynamic entanglement. Exfoliation yield will decrease at a high concentration as partially exfoliated flakes are the main portion of products. The low absorbance intensity observed for graphite powder at 3.0 wt% might be due to the potential error in sample preparation where the presence of the graphite powder was incorporated in the well plate during sample analysis using the UV–Vis spectrometer.

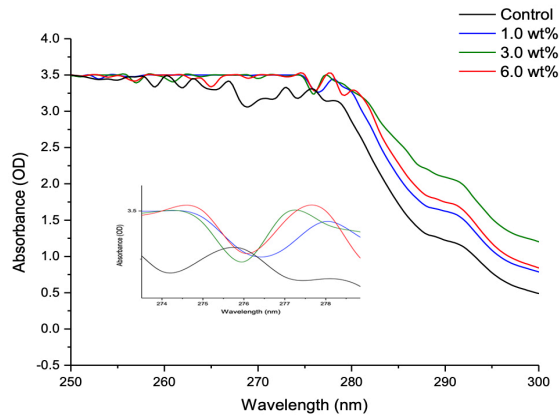


Figure 3: UV absorbance intensity of different weight percentages of liquid-exfoliated graphene in chloroform after sonication at 120 min.

Correlative analysis of BG powder suspended in chloroform prior to the addition of graphite is shown in Figure 4. The absorbance intensity increased within the wavelength ranging from 290 nm to 550 nm as the amount of BG in the chloroform increases from 1.0 wt% to 5.0 wt%. At a higher weight percentage of BG (7.5 wt% and 10.0 wt%), a downturn in absorbance intensity is observed, which is

contributed by BG powder agglomeration caused by the high concentration of BG in chloroform. The dispersion of BG particles is inefficient because of clumps of particles instead of fine-grained suspension dispersed in the solvent. The BG used in the current project was synthesised through a sol-gel method and sieved using a 50-micron sieve. However, the agglomerate clusters of BG particles are still present because of the high concentration of BG particles within the suspension. Furthermore, the presence of energy interaction potential and Van der Waals forces hinders wetting throughout excess BG particles. Hence, in deagglomerating this interaction, high sonication energy is needed for particle dispersal whereby a larger particle size requires greater force for deagglomeration.<sup>25</sup>

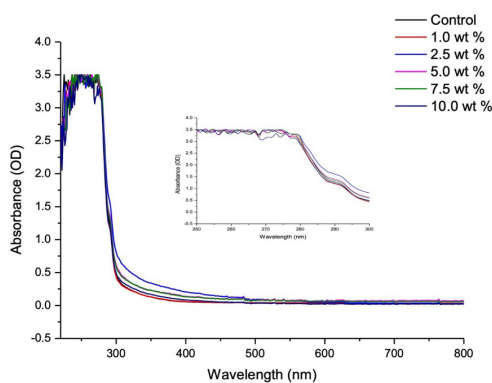


Figure 4: UV absorbance intensity of different weight percentages of BG suspension in chloroform after sonication at 120 min.

As shown in Figure 4, similar to a previous study, UV bands within BG suspensions at approximately 220 nm to 300 nm can be observed, confirming the presence of  $\text{Fe}^{3+}$  and  $\text{Fe}^{2+}$  iron impurities in the emulsion of Bioglass.<sup>26</sup>

### 3.3 Determination of Graphene and BG Concentration in Liquid Suspension

With regard to graphene and BG combination, Figure 5 shows that the concentration of the material mixture increases proportionally to the absorbance intensity, whereas the greatest state and higher intensity occur at 3.0 wt% and 6.0 wt% with combined BG at 2.5 wt% as both suspensions have almost similar absorbance intensity. By contrast, at higher concentrations of BG (5.0 wt%); a slight decrease in absorbance intensity is observed for all concentrations of graphite, which might be due to the agglomeration and precipitation of both constituents and domineering of lower BG absorbency upon addition to graphite.<sup>27</sup> Graphene showed distribution stability following liquid exfoliation in chloroform, which is further enhanced through BG addition in the suspension at a



suitable concentration, because the relationship between these two materials with regard to solubility ratio affects cell responses.

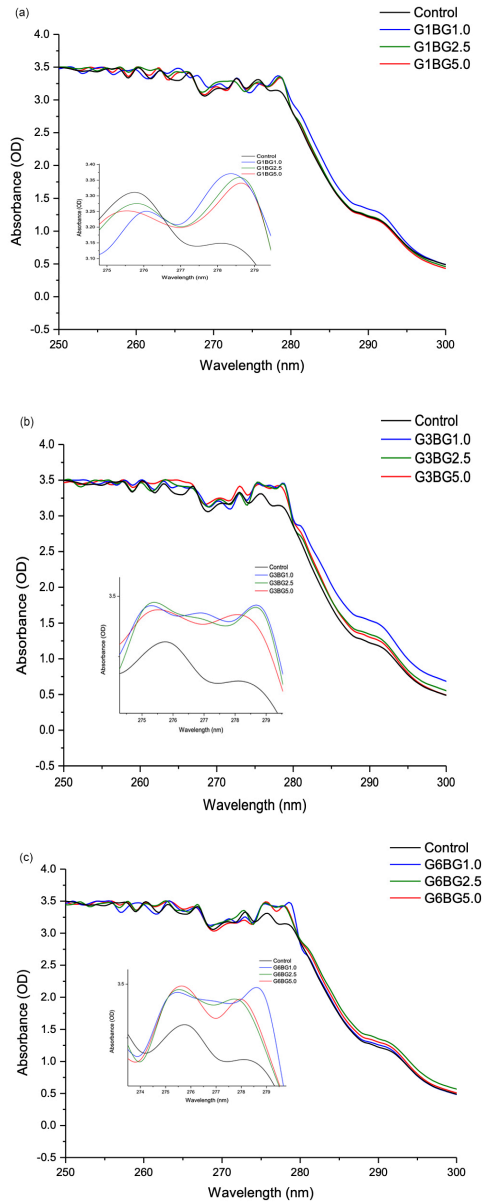


Figure 5: UV absorbance intensity of liquid-exfoliated graphene-BG suspension in chloroform after 120 min of sonication. Different weight percentages of graphite and BG used for comparisons as shown in (a) 1.0 wt%, (b) 3.0 wt% and (c) 6.0 wt% of graphite exfoliated with 1.0 wt%, 2.5 wt% and 5.0 wt% of BG.

Figure 5 shows the interdependent correlation of both materials with the improvement of absorbance intensity following BG addition. This disadvantage can retard the processing ability of these two superior materials. Therefore, the addition of BG in the suspension plays a critical role in improving the solubility and homogeneity properties of graphene in chloroform, which shows great importance to several functional applications.

#### 4. CONCLUSION

The current findings highlight that the sonication time for the production of graphene in chloroform is successful and optimised at 120 min using the LPE method. The peaks of exfoliated graphene suspension are observed at ~279 nm, which is almost similar to pure graphene peaks at ~277 nm–280 nm as shown by UV-Vis spectroscopy. Meanwhile, the absorbance intensity of BG decreases at high concentrations (7.5 wt% and 10.0 wt%) because of the inefficient dispersion of BG particles in the solvent. The incorporation of BG with liquid-exfoliated graphene in a single suspension provides better distribution stability at lower graphene, and BG concentrations with the optimum combination are G3BG2.5 and G6BG2.5, which suggests the exceptional relationship of these two bioactive materials. Hence, this finding could provide an insight for a better biomaterial formulation strategy for diverse application in biomedical and tissue engineering fields.

#### 5. ACKNOWLEDGEMENTS

The authors acknowledged the support from the Ministry of Higher Education Malaysia under the Fundamental Research Grant Scheme (FRGS) No. FRGS/1/2018/STG07/USM/02/13 (203.CIPPT.6711664).

#### 6. REFERENCES

1. Novoselov, K. S. et al. (2004). Electric field effect in atomically thin carbon films. *Science*, 306(5696), 666–669. <https://doi.org/10.1126/science.1102896>
2. Zhao, X. et al. (2010). Enhanced mechanical properties of graphene-based poly(vinyl alcohol) composites. *Macromolecules*, 43(5), 2357–2363. <https://doi.org/10.1021/ma902862u>
3. Cui, X. et al. (2011). Liquid-phase exfoliation, functionalization and applications of graphene. *Nanoscale*, 3(5), 2118–2126. <https://doi.org/10.1039/c1nr10127g>
4. Al Hassan, M. R. et al. (2019). Emergence of graphene as a promising anode material for rechargeable batteries: A review. *Mater. Today Chem.*, 11, 225–243. <https://doi.org/10.1016/j.mtchem.2018.11.006>

5. Nag, A., Mitra, A. & Mukhopadhyay, S. C. (2018). Graphene and its sensor-based applications: A review. *Sens. Actuators A Phys.*, 270, 177–194. <https://doi.org/10.1016/j.sna.2017.12.028>
6. Phiri, J., Gane, P. & Maloney, T. C. (2017). General overview of graphene: Production, properties and application in polymer composites. *Mater. Sci. Eng. B.*, 215, 9–28. <https://doi.org/10.1016/j.mseb.2016.10.004>
7. Cui, G. et al. (2019). A comprehensive review on graphene-based anti-corrosive coatings. *Chem. Eng. J.*, 373, 104–121. <https://doi.org/10.1016/j.cej.2019.05.034>
8. Shen, H. et al. (2012). Biomedical applications of graphene. *Theranostics*, 2(3), 283–294. <https://doi.org/10.7150/thno.3642>
9. Ferrari, A. C. et al. (2015). Science and technology roadmap for graphene, related two-dimensional crystals, and hybrid systems. *Nanoscale*, 7(11), 4598–4810. <https://doi.org/10.1039/C4NR01600A>
10. Uran, S. et al. (2017). Study of ultraviolet-visible light absorbance of exfoliated graphite forms. *AIP Adv.*, 7(3), 35323. <https://doi.org/10.1063/1.4979607>
11. Kumar, N. et al. (2021). Top-down synthesis of graphene: A comprehensive review. *FlatChem*, 27, 100224. <https://doi.org/10.1016/j.flatc.2021.100224>
12. Xu, Y. et al. (2018). Liquid-phase exfoliation of graphene: An overview on exfoliation media, techniques, and challenges. *Nanomater.*, 8(11), 942. <https://doi.org/10.3390/nano8110942>
13. Li, X. et al. (2008). Highly conducting graphene sheets and Langmuir–Blodgett films. *Nat. Nanotechnol.*, 3(9), 538–542. <https://doi.org/10.1038/nnano.2008.210>
14. Hernandez, Y. et al. (2008). High-yield production of graphene by liquid-phase exfoliation of graphite. *Nat. Nanotechnol.*, 3(9), 563–568. <https://doi.org/10.1038/nnano.2008.215>
15. Liscio, A. et al. (2017). Exfoliation of few-layer graphene in volatile solvents using aromatic perylene diimide derivatives as surfactants. *Chempluschem.*, 82(3), 358–367. <https://doi.org/10.1002/cplu.201600503>
16. Ilyas, K. et al. (2019). In-vitro investigation of graphene oxide reinforced bioactive glass ceramics composites. *J. Non Cryst. Solids.*, 505, 122–130. <https://doi.org/10.1016/j.jnoncrysol.2018.10.047>
17. Eqtesadi, S. et al. (2017). Reinforcement with reduced graphene oxide of bioactive glass scaffolds fabricated by robocasting. *J. Eur. Ceram. Soc.*, 37(12), 3695–3704. <https://doi.org/10.1016/j.jeurceramsoc.2016.12.047>
18. Aliaa, N. S. et al. (2019). Synthesis and characterization of PLA-PEG biocomposite incorporated with sol-gel derived 45S5 bioactive glass. *Mat. Today: Proc.*, 17(3), 982–998. <https://doi.org/10.1016/j.matpr.2019.06.466>
19. Durge, R., Kshirsagar, R. V. & Tambe, P. (2014). Effect of sonication energy on the yield of graphene nanosheets by liquid-phase exfoliation of graphite. *Procedia Eng.*, 97, 1457–1465. <https://doi.org/10.1016/j.proeng.2014.12.429>
20. Rotenberg, E. et al. (2008). Origin of the energy bandgap in epitaxial graphene. *Nat. Mater.*, 7(4), 258–259. <https://doi.org/10.1038/nmat2154a>
21. Moosa, A. A. & Abed, M. S. (2021). Graphene preparation and graphite exfoliation. *Turk. J. Chem.*, 45(3), 493–519. <https://doi.org/10.3906/kim-2101-19>

22. Duan, D. et al. (2018). Efficient exfoliation of graphite in chloroform with a pyrene-containing hyperbranched polyethylene as stabilizer to render pyrene-functionalized high-quality graphene. *Carbon*, 136, 417–429. <https://doi.org/10.1016/j.carbon.2018.04.042>
23. Noroozi, M. et al. (2016). Environmental synthesis of few layers graphene sheets using ultrasonic exfoliation with enhanced electrical and thermal properties. *PLoS ONE*, 11(4), e0152699. <https://doi.org/10.1371/journal.pone.0152699>
24. Gomez, V. C. et al. (2021). The liquid exfoliation of graphene in polar solvents. *Appl. Surf. Sci.*, 546, 149046. <https://doi.org/10.1016/j.apsusc.2021.149046>
25. Mittal, G. et al. (2015). A review on carbon nanotubes and graphene as fillers in reinforced polymer nanocomposites. *J. Industr. Eng. Chem.*, 21, 11–25. <https://doi.org/10.1016/j.jiec.2014.03.022>
26. El-Tablawy, S. Y., Abd-Allah, W. M. & Araby, E. (2018). Efficacy of irradiated bioactive glass 45S5 on attenuation of microbial growth and eradication of biofilm from AISI 316 L Discs: In-vitro Study. *Silicon*, 10(3), 931–942. <https://doi.org/10.1007/s12633-017-9550-0>
27. Ma, P. C. et al. (2006). A cohesive law for carbon nanotube/polymer interfaces based on the Van der Waals force. *J. Mech. Phys. Solids*, 54(11), 2436–2452. <https://doi.org/10.1016/j.jmps.2006.04.009>